Journal of Nanobiotechnology

RESEARCH Open Access

Enzyme-armed nanocleaner provides superior detoxification against organophosphorus compounds via a dual-action mechanism

Kang Qin[1†], Fei Meng[2†], Dianpeng Han[1], Wengeng Guo[2], Xinyi Li[1], Ziming Li[1], Lianqun Du[1], Huanying Zhou[1], Hongyuan Yan[2*], Yuan Peng[1*] and Zhixian Gao[1*]

Abstract

By inhibiting acetylcholinesterase (AChE) activity, organophosphate compounds (OPs) can quickly cause severe injury to the nervous system and death, making it extremely difficult to rescue victims after OP exposure. However, it is quite challenging to construct scavengers that neutralize and eliminate these harmful chemical agents promptly in the blood circulation system. Herein, we report an enzyme-armed biomimetic nanoparticle that enables a 'targeted binding and catalytic degradation' action mechanism designed for highly efficient in vivo detoxification (denoted as 'Nanocleaner'). Specifically, the resulting Nanocleaner is fabricated with polymeric cores camouflaged with a modified red blood cell membrane (RBC membrane) that is inserted with the organophosphorus hydrolase (OPH) enzyme. In such a subtle construct, Nanocleaner inherits abundant acetylcholinesterase (AChE) on the surface of the RBC membrane, which can specifically lure and neutralize OPs through biological binding. The OPH enzyme on the membrane surface breaks down toxicants catalytically. The in vitro protective effects of Nanocleaner against methyl paraoxon (MPO)-induced inhibition of AChE activity were validated using both preincubation and competitive regimens. Furthermore, we selected the PC12 neuroendocrine cell line as an experimental model and confirmed the cytoprotective effects of Nanocleaner against MPO. In mice challenged with a lethal dose of MPO, Nanocleaner significantly reduces clinical signs of intoxication, rescues AChE activity and promotes the survival rate of mice challenged with lethal MPO. Overall, these results suggest considerable promise of enzyme-armed Nanocleaner for the highly efficient removal of OPs for clinical treatment.

Keywords Detoxification, Cell membrane coating, Biomimetic nanoparticles, Organophosphate compound, Cytoprotection

[†]Kang Qin and Fei Meng contributed equally to this work.

*Correspondence:
Hongyuan Yan
yanhy@hbu.edu.cn
Yuan Peng
dalidao@139.com
Zhixian Gao
gaozhx@163.com
[1]Tianjin Key Laboratory of Risk Assessment and Control Technology for Environment and Food Safety, Military Medical Sciences Academy, Tianjin 300050, China
[2]Hebei Key Laboratory of Public Health Safety, College of Public Health, Hebei University, Baoding 071002, China

Introduction

Cases of poisoning by lethal chemical substances have become a potent healthcare issue worldwide. Organophosphorus compounds (OPs) are widely used as pesticides, insecticides and even chemical warfare agents [1]. According to the World Health Organization, 200,000 people per year in developing countries died of OPs pesticide poisoning [2]. After OPs exposure, acetylcholinesterase (AChE) is irreversibly inactivated, leading to the accumulation of acetylcholine (ACh). Such accumulation has various neurotoxic effects throughout the nervous system [3]. Although acute lethality can be effectively prevented and intoxication signs can be alleviated after the prompt application of traditional medical countermeasures, including atropine, oxime reactivators and anticonvulsants, the effects of OPs (convulsions, incapacitation, performance deficits, and permanent brain damage) are still devastating [4]. In addition, some serious side effects make the application of these classic antidotes challenging [5]. Therefore, effective detoxification of OPs poisoning is of great importance to human health.

Bioscavenger therapy has emerged as an efficacious countermeasure to detoxify OPs in vivo. In general, these bioscavengers function either by stoichiometric neutralization with OPs (mole-to-mole binding) or by catalytic facilitation of OPs hydrolysis. For instance, the therapeutic potential of the human plasma enzyme butyrylcholinesterase (HuBChE) is derived from the ability of the enzyme to stoichiometrically scavenge OPs nerve agents. Animal studies in guinea pigs have revealed that intravenous administration of large doses of HuBChE confers protection against soman and VX [6]. Furthermore, it has been estimated that 200 mg of HuBChE can protect humans against 2 times the LD_{50} of soman [7]. However, HuBChE has quite a low efficiency in OPs scavenging because of its stoichiometric binding mechanism. The application of high-efficiency catalytic enzymes to hydrolyse OPs in the blood has received broad interest and is considered to be relatively advantageous compared to the use of stoichiometric binding partners [8]. As an organophosphotriester hydrolysing enzyme originally isolated from soil bacteria, organophosphorus hydrolase (OPH) effectively hydrolyses a range of organophosphate esters. However, the OPH enzyme is rapidly cleared by the immune system and exhibits a short circulating half-life (<1 h in rodents) if administered intravenously [9, 10]. Thus, OPH requires extraordinary drug doses and frequent administration, and furthermore, it is unable to exhibit a protective effect. Therefore, there is an unmet need to develop new strategies to improve the catalytic activity and stability of these OPHs in vivo. The urgent need for safe and effective detoxification has prompted the development of OP bioscavengers to neutralize or remove toxicant molecules.

Recently, cell membrane coatings have gained momentum as therapeutic nanotechnologies that endow a series of synthetic materials with cell-like functions, resulting in biomimetic designs with multiple biological functions [11]. Cell membrane-coated nanoparticles inherit the surface merits of source cells and thus bear unique biological functions. For example, nanoparticles coated with red blood cell (RBC)-derived membranes could act as decoys to capture toxic chemical agents, bacterial toxins and pathological autoantibodies [4, 12, 13]. These membrane-coated nanoformulations divert hazardous substances away from and prevent their attack towards healthy RBCs. Furthermore, those cloaked with macrophages, neutrophils and lung epithelial cells can target and absorb a wide range of pathological toxins, proinflammatory cytokines and pathogens [14–16]. The sequestration mechanism by which the membrane endows the nanoparticles for detoxification is the stoichiometric binding between the toxicants and the cell membrane [17]. However, this stoichiometric binding mechanism has quite low efficiency and is unable to achieve high detoxication against lethal organophosphates and other chemicals [18].

To achieve in vivo interception of toxic OPs in the bloodstream, we developed a novel nanoparticle cloaked with an OPH enzyme-armed RBC membrane, herein denoted as 'Nanocleaner', to serve as a bioscavenger against OPs and protect AChE in the peripheral organs and central nervous system. In this study, Nanocleaner provided a dual-modal detoxification, including stoichiometric binding and facilitation of the hydrolysis of OPs that would otherwise attack self-generated RBCs. Using methyl paraoxon (MPO) as the model OP, the dual-action mechanism of Nanocleaner was validated using a series of in vitro assays, including MPO hydrolysis test and AChE protection assays in two regimens. It also shows cytoprotective effects against OP attack in vitro, including maintaining the equilibrium of the mitochondrial membrane potential and attenuating excessive ROS production in the neuroendocrine cell line PC12. In a mouse intoxication model, intravenously injected Nanocleaner efficiently reduced clinical signs of intoxication and improved mouse survival in a dose-dependent manner. In addition, the results of blood cell analysis, comprehensive metabolic panels and histologic examinations of major organs demonstrated that Nanocleaner has satifactory biosafety. The superior detoxification performance and therapeutic potential in treating OP poisoning suggest the great potential of Nanocleaner as a promising bioscavenger.

Materials and methods

Reagents

DSPE-PEG_{2000}-NHS was obtained from Ruixi Biological Technology (Xi'an, China). OPH (EC3.1.8.1, UniProt ID Q5W503) was obtained from Schengenbiya Bioengineering Technology (Beijing, China). Carboxy-terminated poly(D, L-lactide-co-glycolide) acid (PLGA, 50:50, M_W = 15000) was obtained from the Institute of Medical Instruments (Shandong, China). Methyl paraoxon (MPO, purity 98.9%) was obtained from CATO Research Chemicals (Guangzhou, China). Isopore™ hydrophilic polycarbonate porous membranes, polyvinylidene fluoride (PVDF) membranes and Immobilon western chemiluminescent HRP substrate were obtained from Milipore Corporation (Billerica, MA, USA). A bicinchoninic acid (BCA) assay kit, a cell plasma membrane staining kit with 1,1'-dioctadecyl-3,3,3',3'-tetramethylindocarbocyanine perchlorate (DiI), 1,1'-dioctadecyl-3,3,3',3'-tetramethylindodicarbocyanine, 4-chlorobenzenesulfonate salt (DiD) and a mitochondrial membrane potential assay kit with 5',6,6'-tetrachloro-1,1',3,3-tetraethylbenzimidazolylcarbocyanine iodide (JC-1) were obtained from Beyotime Biotechnology (Shanghai, China). A gel fast preparation kit and multicolor prestained protein ladder were obtained from Epizyme Biomedical Technology (Shanghai, China). Anti-CD47 (ab218810) and anti-GAPDH (ab185059) goat anti-rabbit IgG H&L (HRP) (ab205718) antibodies were obtained from Abcam (Cambridge, UK). WB ultrasensitive ECL luminescent liquid was obtained from Invigentech (CA, USA). Fluorescein isothiocyanate, isomer 1 (FITC) was obtained from Heowns Biochemical Technology (Tianjin, China). Acetylthiocholine iodide was obtained from Sigma-Aldrich (MO, USA). 5,5'-Dithiobis-(2-nitrobenzoic acid) (DTNB) was obtained from BioRuler (CT, America). Dulbecco's modified Eagle's medium/nutrient mixture F-12 (DMEM/F-12, 11330-032), fetal bovine serum (FBS) and horse serum were obtained from Gibco (NY, USA). A cell counting kit-8 (CCK-8) was obtained from Biosharp (Anhui, China). 2',7'-Dichlorodihydrofluorescein diacetate (DCFH-DA) was obtained from MedChemExpress (NJ, USA). The optimal cutting temperature compound (O.C.T.) was obtained from Sakura Tissue-Tek (USA). H&E staining kit was obtained from Leagene Biotechnology (Beijing, China). All other chemical reagents were obtained from Chemical Reagent Company (Tianjin, China).

Animal use and care

Male ICR mice (6−8 weeks old, 20–25 g) were purchased from HFK Bioscience. Co., Ltd. (Beijing, China). The use of experimental mice was approved by the Animal Experiments Ethical Committee of the Tianjin Institute of Environmental and Operational Medicine. Animals were housed in individually ventilated cages (IVC) and were provided food and water.

Derivation of mouse erythrocyte membranes

The RBC membranes were obtained according to a previous report [4]. Briefly, collected mouse RBCs were washed with cold 1 × PBS three times at 800 × g for 5 min and then suspended in hypotonic 0.25 × PBS on ice for 20 min for hemolysis using refrigerated microcentrifuges (Microfuge 20R, Beckman Coulter Life Science, USA). The mixture was then centrifuged at 10,000 × g for 5 min. The hypotonic treatment was repeated three times, and the pink RBC ghosts were collected. The collected membrane was aliquoted and stored at -80 °C for subsequent studies. The membrane protein concentration was quantified by a BCA protein assay kit. One milliliter of whole blood yielded approximately 6 mg of cell membrane (protein weight).

OPH conjugation on RBC membranes

OPH was conjugated to the DSPE-PEG_{2000}-NHS linker according to a previous report with slight modifications [19]. Briefly, 50 mg of OPH was dispersed in 50 mL of PBS, fully dissolved and transferred to a reaction flask. Subsequently, 250 mg of DSPE-PEG_{2000}-NHS was added, and the mixture was stirred overnight at 4 °C. Finally, the unreacted DSPE-PEG_{2000}-NHS and free OPH were removed by ultrafiltering and washing 3 times using an Amicon centrifugal filter device (Millipore, UFC901096, USA) with a MWCO of 10 kDa at 4 °C for 15 min. The purified DSPE-PEG-OPH and OPH were analysed by native PAGE. Fourier transform infrared (FT-IR) spectra of DSPE-PEG-OPH, DSPE-PEG-NHS and OPH were collected and compared using OMNIC Mercury TGA software (Nicolet™ iS50 FT-IR, Thermo Scientific, USA).

Then, the OPH enzyme-armed RBC membrane was prepared by mixing the DSPE-PEG-OPH solution and RBC membrane suspension, followed by incubation at 4 °C for 24 h. The mixture was washed 3 times with PBS to remove unbound DSPE-PEG-OPH and free OPH. To further concentrate the OPH-armed RBC membranes, the mixture was further centrifuged at 10,000 × g at 4 °C for 15 min, followed by washing and resuspension in 2 mL of PBS.

To obtain an optimized input concentration, RBC membranes and DSPE-PEG-OPH conjugates were mixed in different proportions (10:1, 10:2, 10:4, 10:6 and 10:8, w/w). After modification, the activities of the OPH-RBC membrane conjugates were calculated according to the concentration of *para*-nitrophenol (PNP). In brief, 100 μL of OPH-RBC membrane conjugates (0.4 mg/mL) and 100 μL of MPO (0.25 mg/mL) were added to 300 μL of HEPES buffer solution (pH 8.0, 50 mM). After being incubated at 37 °C for 5 min and 15 min, the reaction was

terminated by the addition of 100 μL trichloroacetic acid (TCA, 10 wt%) in an ice and water bath. The mixture was immediately centrifuged (10,000 × g) at 4 °C. Then, 50 μL of Na_2CO_3 (10 wt%) was added to 300 μL of the supernatant for colorimetric detection at 409 nm.

Preparation of nanocleaner

Biodegradable PLGA nanoparticles were prepared by a nanoprecipitation method reported previously [20]. First, 50:50 carboxy-terminated PLGA was dissolved in acetone at a concentration of 10 mg/mL. A 1 mg/mL solution was rapidly added to 3 mL of ultrapure water. To remove the acetone, the solution was stirred for 2 h and then placed in a 25 °C vacuum drying oven for 8 h. The solution of the nanoparticle suspensions was adjusted to 1 × PBS using 10 × PBS. Then, the PLGA solution was mixed with a suspension containing OPH enzyme-armed RBC membranes (polymer: membrane protein weight ratio = 1:1). The mixture was then sonicated for 15 min on a probe sonicator (SCIENTZ-750 F, Ningbo Scientz Biotechnology, China) at a power of 105 W with 2 s on and 1 s off and subsequently extruded sequentially through 400 and 200 nm polycarbonate porous membranes (Millipore, USA) on an extruder (Nayi Instrument Technology, China) to form Nanocleaner. To determine the content of OPH enzyme on the Nanocleaner, the mixture was centrifuged and ultrafiltered to collect nanoparticles and the concentration of unbound OPH molecules in the supernatants was calculated according to the concentration of its catalytic product at 409 nm. Nanocleaner was resuspended in PBS solution (1×) and then injected intravenously for in vivo treatment with MPO intoxication. For the preparation of RBC-NPs, RBC membranes and PLGA cores were mixed, sonicated and extruded as described above.

To determine whether OPH conjugates were anchored on the membranes, OPH was fluorescently labelled with FITC dye (green) according to a previous study [21] and then conjugated with DSPE-PEG_{2000}-NHS. Meanwhile, RBC membranes were labelled with DiI dye (orange red) following the vendor's protocol. For the preparation of fluorescently labelled Nanocleaner, dye-labelled RBC membranes and DSPE-PEG_{2000}-OPH-FITC were mixed, washed, sonicated and extruded. The Nanocleaners labelled with dual immunofluorescence were immobilized in glycerol and visualized on a laser scanning confocal microscope (LSCM, Zeiss LSM710, Germany).

Physicochemical characterization

To further confirm the coating, nanoparticles were stained with uranyl acetate and visualized using transmission electron microscopy (TEM, FEI 200X, USA) to visualize the core-shell structure.

The hydrodynamic diameter, polydispersity index (PDI) and surface ζ potential of Nanocleaner with a suitable concentration were measured via dynamic light scattering (DLS, NanoBrook 90Plus PALS, USA). The colloidal stability of Nanocleaner was examined in 1 × PBS, followed by measuring the sizes for 5 consecutive days. PLGA NP and RBC-NP served as controls.

Gel electrophoresis and western blotting

Native-PAGE was performed using a 10% separating gel, and the gels were stained with Coomassie blue dye and discoloured with a methanol solution-acetic acid mixture and deionized water.

To confirm the presence of CD47 on the surface of the nanoparticles, anti-CD47 antibodies were used for western blotting. Samples containing RBC ghosts, RBC-NP, and Nanocleaner were denatured in protein sample buffer containing 2-mercaptoethanol, a reducing agent, and loaded on an 8% polyacrylamide gel in Tris-glycine (Laemmli) SDS running buffer. The samples were run at 80 mV for 20 min and 120 mV for 60 min. The proteins were then transferred onto polyvinylidene fluoride (PVDF) membranes at 220 mA for 80 min, blocked with milk at 25 °C for 1 h, and incubated with the primary antibodies CD47 and GAPDH at 4 °C overnight. Finally, the PVDF membranes were further incubated with a rabbit anti-mouse IgG horseradish peroxidase (HRP) conjugate. The stained PVDF membrane was subjected to enhanced chemiluminescence (ECL) and photographed by a bolt and gel imager (Amersham Imager 680, General Electric Company, USA).

In vitro hydrolase activity

3 mL of aqueous PBS solution (1 ×) containing MPO (1 mg/mL) Nanocleaner at various concentrations (0.01-1 mg/mL) was incubated at 37 °C, and 1 mg/mL RBC-NP and 6.08 nmol/mL free OPH were used as controls. At each predetermined time point, 50 μL of solution was collected and diluted by the addition of 150 μL of PBS. The reaction was then terminated by the addition of 100 μL of trichloroacetic acid (10% w/v) and centrifuged at 14,000 rpm at 4 °C for 5 min. Then, 50 μL of Na_2CO_3 (10% w/v) was introduced into 100 μL of the supernatant for colorimetric reaction. The absorbance of the supernatant at 409 nm was recorded by using a μQuant microplate spectrophotometer (BioTeK, USA). The absorbance and catalytic product amount were determined according to standard curves.

In vitro protection of AChE against MPO

The half maximal inhibitory concentration (IC_{50}) was first identified as the concentration at which MPO inhibited 50% of AChE activity in RBC ghosts. One hundred microliters of PBS (1 ×, pH 7.4) containing 2.5% (v/v)

RBC ghosts was mixed with various concentrations of MPO solution. AChE activity was plotted and fitted with a dose–response–inhibition curve. To investigate the protective effect of Nanocleaner on AChE activities under MPO exposure, tests were carried out with two regimens. In a preincubation regimen, 10 μL of MPO solution (final concentration: 1.435 mg/mL) was mixed with 100 μL of nanoparticles at various concentrations. After incubation for 15 min, the solutions were centrifuged at 14,000 × g for 30 min, and the nanoparticles were removed. 90 μL of supernatant was collected, added to 10 μL of 2.5% (v/v) RBC ghost and incubated at 37 °C for 30 min. Pellets of RBC ghost were collected by centrifugation at 2000 rpm for 10 min to measure AChE activity.

In a competitive regimen, 100 μL of PBS (1 ×, pH 7.4) containing 4 mg/mL Nanocleaner and 2.5% (v/v) RBC ghosts was incubated with a gradient concentration of MPO at 37 °C for 30 min. RBC ghosts were pelleted and harvested by centrifugation at 2000 rpm for 10 min, while the supernatant containing nanoparticles and MPO was discarded.

The AChE activity assay was based on Ellman's method described in a previous report [22, 23]. The pellets of fresh RBC ghosts were suspended in 100 μL of PBS. Then, 40 μL of RBC membrane resuspension solution and 60 μL of aqueous working solution (50 mM Tris-HCl, 20 mM KCl, 2 mM DTNB, and 2 mM acetylthiocholine iodide) were added to a 96-well plate, and the absorbance of each well at 412 nm was recorded at the beginning and end of incubation at 37 °C for 20 min.

Hemolytic test

In brief, 100 μL of nanoparticles (4 mg/mL) was added to 100 μL of fresh red blood cells from mice, and the volume was adjusted to 1 mL with sterile PBS (1 ×, pH 7.4). One hundred microliters of blood mixed with 900 μL of PBS served as the negative control, and an equivalent volume of blood mixed with 900 μL of PBS containing 100 mg of ammonium chloride was used as the positive control. After incubation at 37 °C for 90 min, the solutions were centrifuged at 10,000 × g for 10 min. The absorbance at 543 nm was recorded using a plate reader.

In vivo treatment with MPO intoxication

The lethal dose 100% (LD_{100}) was determined by observing the survival of ICR mice after 30 min of treatment with various doses of MPO (2.7-3.0 mg/kg) via intraperitoneal injection. To examine the therapeutic efficacy of Nanocleaner, the mice randomized to three groups of 6 mice. Each group of mice was intraperitoneally administered with MPO at an LD_{100} (2.9 mg/kg). After MPO exposure, Nanocleaner treatment group immediately received a tail vein intravenous injection of 50–200 mg/kg of Nanocleaner, while the RBC-NP treatment group received 50–100 mg/kg of RBC-NP. The control group received an equivalent amount of saline. In addition, according to the quantitative results of OPH content on the Nanocleaner, OPH group received injection of OPH (340.28, 608.57 and 1217.14 nmol/kg).

Typical symptoms of MPO poisoning and survival rate were monitored. The scoring criteria for the intoxication score are shown in Table S1, in which each syndrome contributes a score of 1, with a maximum score of 4. In addition, 50 μL of blood was collected from each mouse by puncturing the retro-orbital venous plexus 15 min after MPO injection or cardiac puncture immediately after death. RBC ghosts were then derived from the collected blood, and the AChE activity of 10 μL of RBC ghosts was measured and compared to that of normal mice.

Cell cultures

The PC12 neuroendocrine cell line was cultured in Dulbecco's modified Eagle medium/nutrient mixture F-12 (DMEM/F-12) medium supplemented with 1% penicillin–streptomycin solution, 5% fetal bovine serum (FBS) and 5% house serum at 37 °C with 5% CO_2 in a constant temperature incubator.

In vitro cytotoxicity assay

A cell counting kit-8 (CCK-8) assay was utilized to determine the cytotoxicity of Nanocleaner and RBC-NP over the course of 12 h. PC12 cells (3×10^4, 100 μL) were seeded into 96-well plates (coated with poly-L-lysine) and cultured at 37 °C with 5% CO_2 for 24 h. Then Nanocleaner and RBC-NP in different concentrations were added, and the cells were cocultured for 12 h. Then, the medium was removed, and 100 μL of medium containing 10% CCK-8 (v/v) was added to each well. After incubating for 1 h, the OD_{450} was recorded in a microplate reader. Cell viability (%) = ($A_{Treated}$-A_{blank}/$A_{control}$- A_{blank}) × 100%, where A_{blank} is the absorbance of medium containing CCK-8, and $A_{Treated}$ and $A_{Control}$ represent the absorbance values with and without Nanocleaner treatment and RBC-NP, respectively.

Mitochondrial membrane potential assay

PC12 cells were seeded on top of poly-l-lysine-coated glass coverslips (ϕ=15 mm, NEST Biotechnology, Wuxi, China) in 24-well plates at a density of 2.5×10^5 cells per well. The plates were placed into a CO_2 incubator and incubated for 24 h to firmly attach to the coverslips. Subsequently, the cells were incubated in 500 μL of medium supplemented with MPO (5 μg/mL), MPO (5 μg/mL)+Nanocleaner (50, 500 μg/mL) or MPO (5 μg/mL)+RBC-NP (50, 500 μg/mL) for 6 h. Blank medium without MPO or nanoparticles served as the control group. After the medium was removed, JC-1 dye was

added, and the cells were incubated and washed according to the manufacturer's instructions. Green and red fluorescence images were recorded and visualized using a fluorescence microscope (Leica DM4B, Germany). The fluorescence intensity was quantified by ImageJ (NIH, USA).

Intracellular ROS detection

PC12 cells (0.5 mL, 2.5×10^5 cells) were seeded on coated glass coverslips for 24 h. After incubation with MPO (5 μg/mL), MPO+Nanocleaner, or MPO+RBC-NP for 6 h, the PC12 cells were stained with a 10 μM DCFH-DA ROS probe for 20 min and visualized using a fluorescence microscope.

In vivo retention and biodistribution of nanocleaner

The nanoparticles were labelled with DiD for the biodistribution test. In brief, Nanocleaner and RBC-NP were incubated with 10 μM DiD for 30 min at 37 °C, respectively. A total of 180 μL of DiD-labelled Nanocleaner or RBC-NP were intravenously administered to the mice at 8 mg/mL. The fluorescence signal at different intervals (3, 24, 48, and 72 h) was observed using a Maestro in vivo optical imaging system (Calliper Life Sciences, USA). At 72 h postadministration, organs, including the heart, liver, spleen, lung and kidney, were harvested and weighed, and the fluorescence signals were recorded. The resulting signal was normalized to the organ weight.

In vivo toxicity of nanocleaner

To assess acute toxicity, 15 mg/mL Nanocleaner was given intravenously through the tail vein to the mice at 100 mg/kg. At 24 h after injection, whole blood from the eyes was sampled into a microcentrifuge tube and allowed to coagulate. The sample was centrifuged at 3000 rpm for 10 min, and the supernatant was centrifuged at 12,000 rpm for 10 min again. Completely separated serum from the top of the sample was used for the comprehensive metabolic panel (CMP). In addition, 100 μL of whole blood was collected for complete blood analysis. Serum and whole blood samples were analysed using an automated haematology analyser (BC-5100, Mindray, China) and a fully automatic biochemical analyser (BS-350E, Mindray, China), respectively. At 72 h postinjection, the mice were sacrificed. The major organs (heart, liver, spleen, lung, and kidney) were fixed, frozen, sectioned at a thickness of 6–8 μm, and stained with hematoxylin-eosin (H&E).

Statistical analysis

All the quantitative results were obtained from at least three samples for data analysis. The data are shown as the mean±standard error of the mean (s.e.m.). GraphPad Prism Software Version 9.0 (CA, USA) was used for statistical analysis. Two groups of comparisons were carried out using Student's t test. Multiple comparisons were performed using one-way analysis of variance (ANOVA). The log-rank (Mantel–Cox) test was used to compare survival data.

Results and discussion

Physicochemical characterization

A novel nanoparticle cloaked with an OPH enzyme-armed RBC membrane (denoted as 'Nanocleaner') was fabricated, as shown in Fig. 1a. With the assistance of abundant AChE and enzyme molecules on the surface, Nanocleaner could compete with host cells and protect AChE from OP intoxication by targeted binding and catalytic degradation (Fig. 1b). To fabricate RBC membrane-coated nanoparticles, RBC membranes were first collected using an established process involving hypotonic treatment and successive centrifugation and then verified for purity. The polymeric cores were prepared using poly(lactic-co-glycolic) acid (PLGA) through a nanoprecipitation method [20]. Finally, RBC membranes were coated onto the PLGA cores via sonication and physical extrusion.

As a medium with editable modifications, DSPE-PEG polymers have been extensively used for medical applications [24–26]. To introduce OPH onto the surface of the RBC membrane, the NHS-terminated DSPE-PEG polymer was covalently bonded to the OPH enzyme through the reaction of active esters with amino groups (Fig. 2a). Native PAGE was performed to confirm the successful conjugation of the NHS-terminated DSPE-PEG linker with the OPH enzyme (Fig. 2b). The movement of enzymes became observably slow after the polymer modification. Compared with those of native OPH, the enzyme-polymer building blocks were further confirmed due to the presence of discrete, free protein bands in the gels. FTIR was used to observe the OPH before and after DSPE-PEG-NHS modification (Figure S1). The peak at 3286 cm^{-1} was attributed to the stretching vibration of N-H, and the peak at 1650 cm^{-1} was attributed to the stretching vibration of C=O. The above peaks were characteristic of OPH and were observed for the product DSPE-PEG-OPH, which indicated the successful preparation of DSPE-PEG-OPH. Furthermore, the peak at 1738 cm^{-1} was attributed to the C=O stretching vibration of the active ester in DSPE-PEG-NHS, and this peak disappeared for the DSPE-PEG-OPH product, indicating that DSPE-PEG-OPH was obtained through the reaction of activated NHS esters of DSPE-PEG-NHS with primary amines of OPH under physiological conditions to produce stable amide bonds.

The synthesized DSPE-PEG-OPH was then introduced to RBC membranes by the interaction between DSPE chemical groups and phospholipid bilayer membranes.

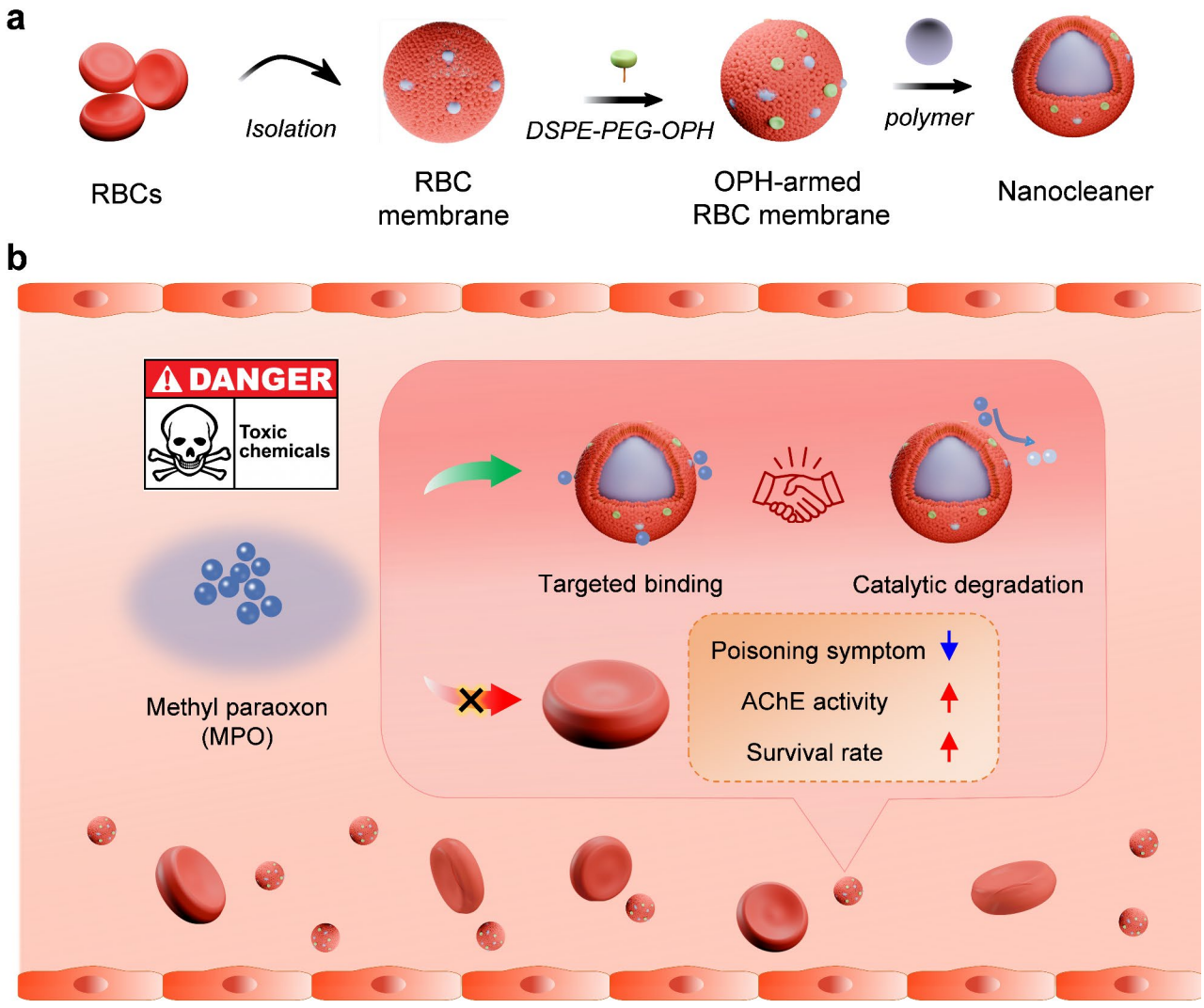

Fig. 1 Schematic illustration of OPH enzyme-armed Nanocleaner for bimodal detoxification of methyl paraoxon (MPO). (**a**) Design and fabrication of Nanocleaner made with polymer nanoparticles wrapped with modified RBC membranes armed with OPH enzyme. (**b**) Nanocleaner, displaying abundant AChE decoys and OPH enzymes on its surface, competes with host cells in the blood and preserves their AChE against MPO intoxication by concurrent targeted binding and catalytic degradation

To confirm that OPH enzymes were indeed located on cell membranes, RBC membranes and enzymes were labelled with fluorescent dyes of two different colors. When observed under a confocal fluorescence microscope, significant fluorescence signal overlap was detected (Fig. 2c). It has been reported that the inner polymeric core could stabilize the RBC membrane shell [27]. The pristine and enzyme-armed RBC membranes were then coated onto polymeric PLGA nanoparticle cores through an ultrasonic-assisted extrusion method to formulate RBC-NP and NanocleanerN, respectively. RBC-NP and Nanocleaner were further examined via transmission electron microscopy (TEM). Under the microscope, Nanocleaner had a spherical core-shell structure, similar to that of conventional RBC-NP (Fig. 2d). Dynamic light scattering (DLS) revealed that upon enzyme-armed membrane coating, the average diameter of Nanocleaner increased ~ 20 nm with a narrow size distribution, which was consistent with the coating of RBC membranes onto bare PLGA-NP. However, the RBC-NP were relatively large (Fig. 2e), possibly because of the mechanical rigidity of the pure RBC membrane [20].

Compared with that of the PLGA-NP, the ζ potential value of the RBC-NP increased by 10 mV, which could be attributed to surface charge shielding caused by the RBC membrane coating [13]. However, the potential value of Nanocleaner decreased and became more negative (~ 7 mV vs. RBC-NP) (Fig. 2f), which was likely due to the association of the RBC membrane with OPH, a negatively charged acidic protein.

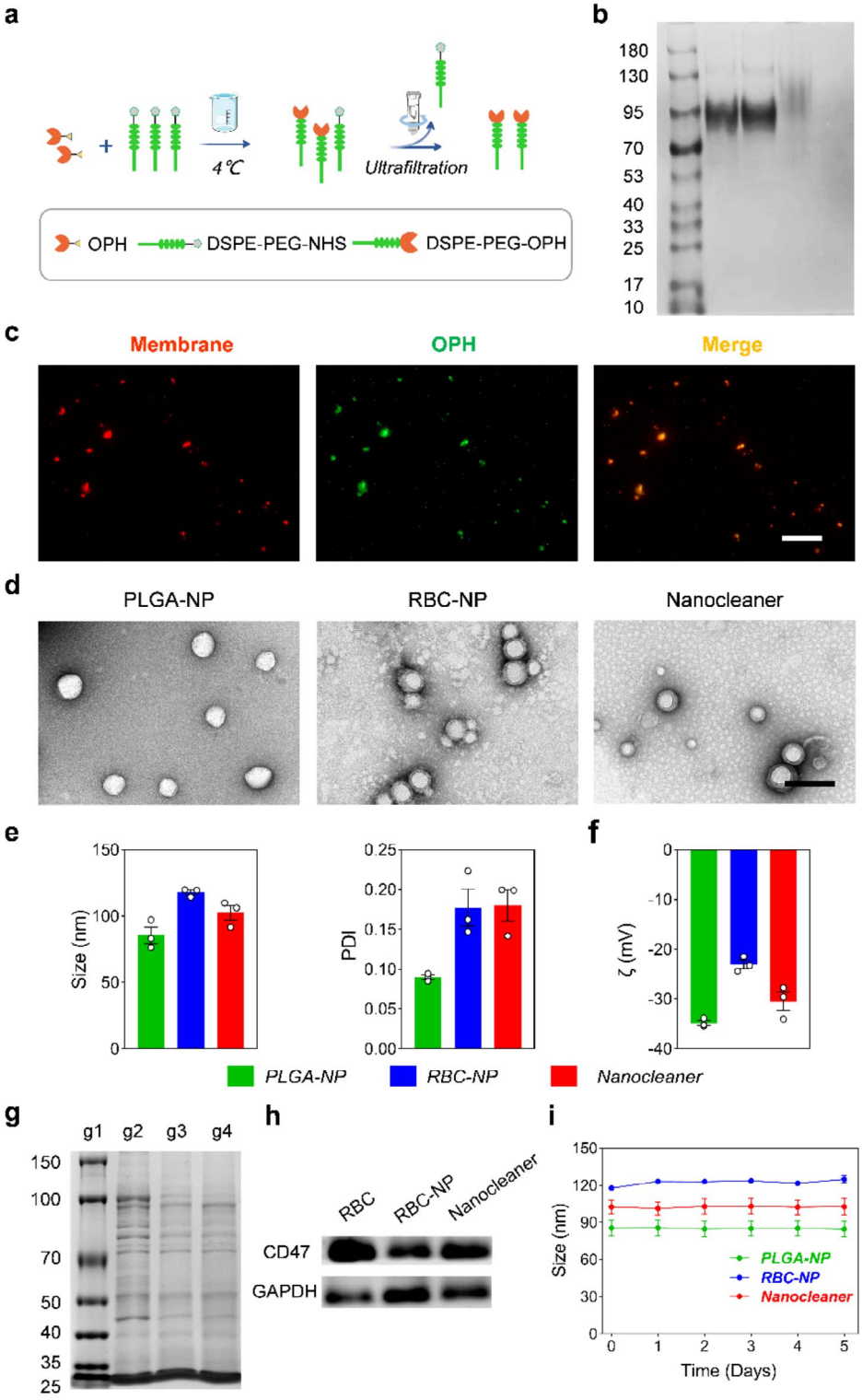

Fig. 2 Fabrication and physicochemical characterization of Nanocleaner. (**a**) Schematic showing the synthesis of DSPE-PEG-OPH. (**b**) DSPE-PEG-OPH was analysed by native PAGE. Left to right: Ladders, OPH (native), OPH (sham), DSPE-PEG-OPH, DSPE-PEG-NHS. (**c**) Confocal fluorescence images of dye-labelled OPH/RBC-NP (RBC membrane, red; OPH, green). (Scale bars, 25 μm). (**d**) TEM images of PLGA-NP, RBC-NP and Nanocleaner. (Scale bars, 200 nm). (**e**) Size, polydispersity index, and (**f**) ζ potential of the nanoparticles ($n = 3$). (**g**) The protein profile of the cell membrane analysed by SDS-PAGE. Left to right: marker (g1), RBC ghost (g2), Nanocleaner (g3) and RBC-NP (g4). **(h)** The presence of RBC membrane-specific CD47 was detected by western blot. (**i**) Long-term stability of nanoparticles in 1 × PBS, monitored over 5 days ($n = 3$)

After being coated onto the nanoparticles, the protein composition of the cell membrane was well retained (Fig. 2g), indicating that the Nanocleaner inherited complex antigenic information and surface properties from the RBC ghost. Furthermore, the CD47 protein, a specific "self-marker" on the RBC membrane, was still present to prevent clearance by the immune system (Fig. 2h) [28].

To investigate the stability of the nanoparticle solutions, the samples were dispersed in PBS, stored at 4 °C and measured by DLS at predetermined time points. The diameters of the PLGA-NP, RBC-NP and Nanocleaner remained stable throughout the entire observation period (Fig. 2i), demonstrating good stability of these nanoparticles. These results suggested that cell membrane coating and modification did not alter the colloidal stability of the nanoformulation.

In vitro catalytic properties

We further examined the catalytic properties of Nanocleaner, which was fabricated with various input concentrations of OPH-RBC membrane protein (weight to weight). A series of input concentrations (1:10, 2:10, 4:10, 6:10 and 8:10) were assessed through a systematic optimization process (Figure S2). As the proportion of OPH increased, the absorbance increased. Considering in vitro catalytic performance, the ratio of OPH to RBC membrane protein (4:10), was selected as the optimal ratio and utilized for subsequent experiments. The result of a catalytic experiment showed that the content of OPH on the Nanocleaner (1 mg/mL) was approximate 6.08 nmol/mL.

OPs are bound to the active metal center of OPH, and the P-O bonds are broken by proton-assisted nucleophilic attack [29, 30], by which MPO is hydrolysed into *para*-nitrophenol (PNP) and phosphonic acid dimethyl ester (Fig. 3a). Then, the generated PNP was detected spectrophotochemically, and a standard curve of PNP concentration was plotted to further quantify PNP concentration during MPO hydrolysis by OPH (Fig. 3b). To confirm the contribution of OPH anchored on Nanocleaner, time- and concentration-dependent hydrolysis experiments of MPO were carried out (Fig. 3c). The results demonstrated that the concentration of generated PNP increased as Nanocleaner concentration increased (from 0.001 to 1 mg/mL). PNP-generating properties were relatively smooth, with a steady increasing trend

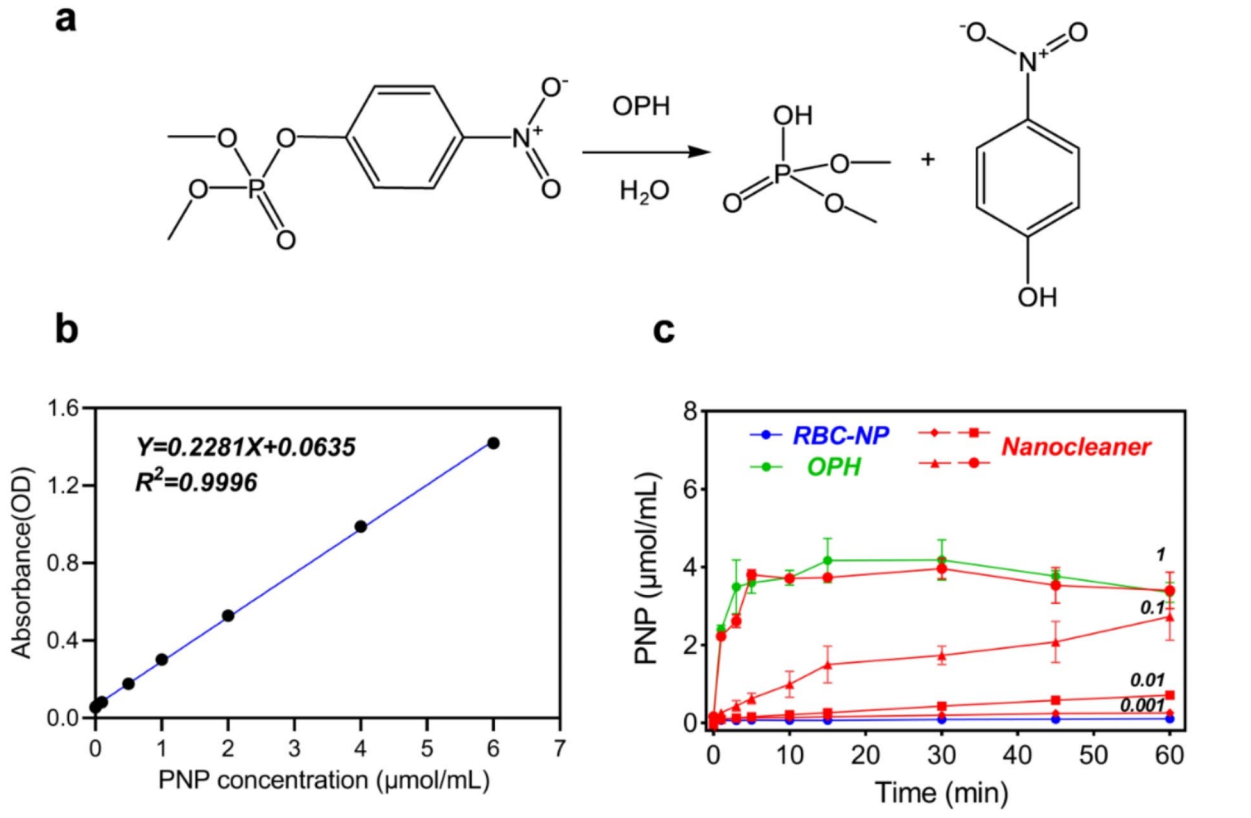

Fig. 3 Catalytic properties of Nanocleaner facilitating OP hydrolysis. (**a**) Reaction process of the hydrolysis of methyl paraoxon by OPH. (**b**) Standard curve of PNP measured spectrophotometrically. (**c**) PNP release in the RBC-NP (1 mg/mL), OPH (6.08 nmol/mL) and Nanocleaner (0.001, 0.01, 0.1 and 1 mg/mL) groups at pH 7.4 ($n = 3$). The data are presented as the mean ± s.e.m. for each group

that eventually reached a plateau after 30 min in the Nanocleaner group. Impressively, the release kinetics of PNP in the 1 mg/mL Nanocleaner group were quite similar to those in the group hydrolysed by free OPH (6.08 nmol/mL), which demonstrated the excellent catalytic activity of Nanocleaner. In contrast, no release of PNP could be observed in the presence of RBC-NP as RBC membranes are unable to hydrolyse MPO catalytically.

Substrate concentration is an important factor to evaluate the free enzyme activity. To compare the catalytic performance and mechanism of OPH with Nanocleaner, a typical Michaelis-Menten curve was obtained at equimolar OPH (Figure S3a and S3b). When the MPO concentration was sufficiently high, we observed increased enzyme activity by occupying active site. The steady-state kinetic parameters V_{max} and K_m were calculated (Figure S3c and S3d) and summarized in Table S2 using the Lineweaver-Burk double-reciprocal plotting method. As Michaelis constant, K_m represents the substrate affinity of the enzyme. The higher the K_m value is, the less affinity of enzymes for the substrate is, and vice versa. V_{max} represents the reaction rate when the enzyme is saturated with substrate, and a higher V_{max} value indicates an improved reaction rate. Therefore, the experimental data showed that the OPH on the surface of Nanocleaner have a higher affinity for MPO than the free OPH and a decreased V_{max} value means less active site. Meanwhile, the reduction of first-order rate constant (k_{cat}) and second-order rate constant (k_{cat}/K_m) demonstrated that catalytic efficiency slightly decreased.

At a concentration of 4 mg/mL, Nanocleaner had almost no loss of activity after 10 freeze-thaw cycles, and over 90% of the activity of Nanocleaner was maintained after storage at 4 °C for 7 days (Figure S4).

In vitro neutralization of MPO

We then investigated the in vitro protective effects of Nanocleaner against MPO-induced inhibition of AChE activity by two regimens. As shown in Fig. 4a, a preincubation regimen was established in which various concentrations of nanoparticles (RBC-NP or Nanocleaner) were thoroughly mixed with MPO, and then RBC ghosts were

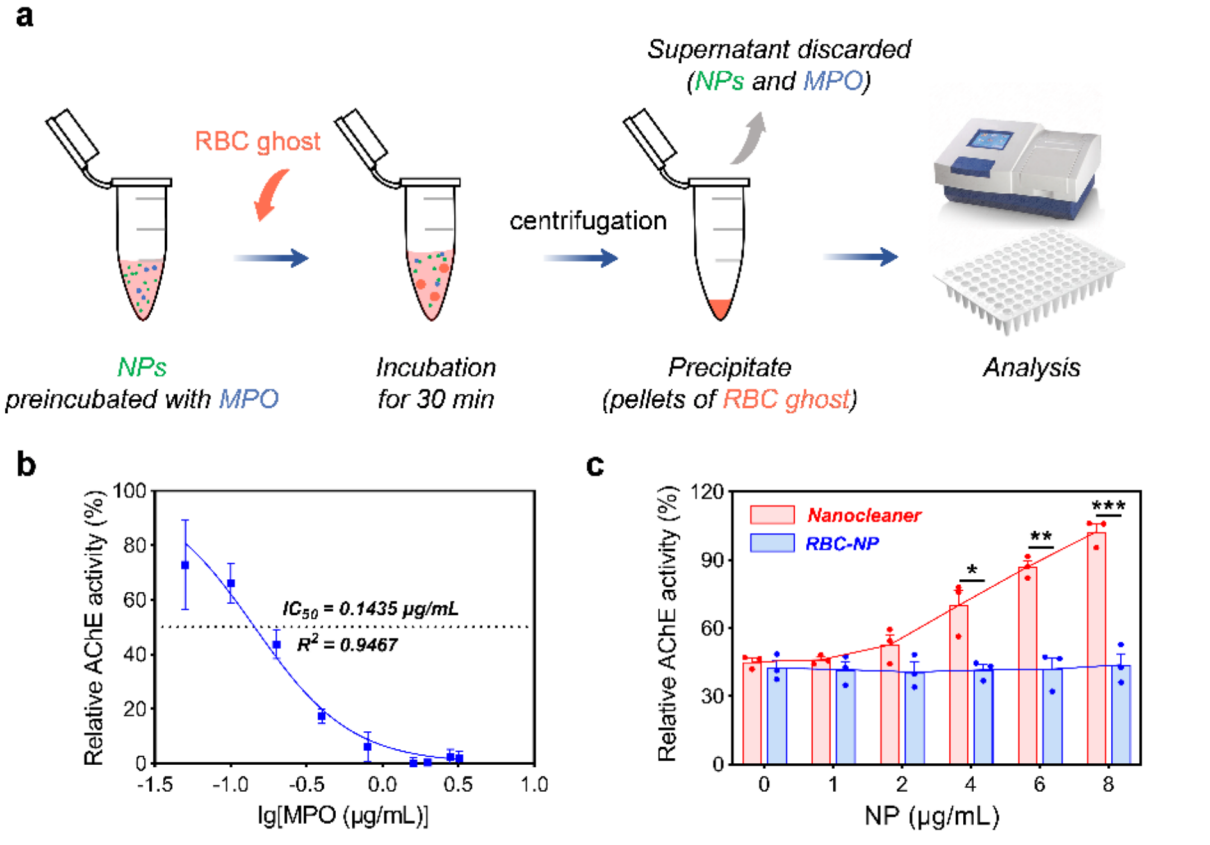

Fig. 4 In vitro neutralization efficacy of Nanocleaner against MPO in a preincubation regimen. (**a**) Schematic depicting the experimental design used to evaluate AChE protection by Nanocleaner. (**b**) Quantification of the remaining AChE activity after incubation of RBC ghosts with various concentrations of MPO and calculation of the half maximal inhibitory concentration (IC_{50}) of MPO against AChE activity ($n = 3$). (**c**) Quantification of the remaining AChE activity of RBC ghosts in the presence of MPO (IC_{50} value) preincubated with various concentrations of RBC-NPs and Nanocleaner for 30 min ($n = 3$). The data are presented as the mean ± s.e.m. for each group. *$p < 0.05$, **$p < 0.01$, ***$p < 0.001$

added to the above mixture. Before preincubation, the AChE-inactivating effects were established. Specifically, RBC ghosts were incubated with various concentrations of MPO, after which the relative AChE activity was measured. After the introduction of MPO, the AChE activity of the RBC ghosts significantly decreased. The values presented a sigmoidal curve as a function of the logarithm of the toxic OP concentration. It could be estimated that when the concentration of MPO was 0.1435 μg/mL, the relative AChE activity decreased to 50% of the initial activity (IC_{50}, Fig. 4b). Then, we mixed different concentrations of nanoparticles (RBC-NP or Nanocleaner, respectively) with 0.1435 μg/mL MPO (IC_{50}). Next, fresh RBC ghosts were added to the mixtures at a final concentration of 2.5% (v/v), after which the relative AChE activity of the RBC ghost was detected. The results showed that the relative AChE activity progressively increased with increasing concentrations of Nanocleaner (Fig. 4c), while the RBC-NP had no positive effect on the recovery of AChE activity because of the small amount of AChE on the surface of the RBC-NP. These AChE enzymes were insufficient for neutralizing high-dose MPO. This finding also indicated that a small amount of AChE decoy had no advantage in terms of neutralization. Impressively, 8 μg/mL Nanocleaner salvaged almost 100% of the AChE activity, indicating that the introduction of the OPH enzyme effectively enhanced the removal of OP. Taken together, these data showed that Nanocleaner neutralized MPO in a concentration-dependent manner. The introduction of OPH remedied the weakness of competitive neutralization at low doses.

Nanocleaner was further examined for its ability to protect against MPO-induced inhibition of RBC AChE in a competitive regimen (Fig. 5a), where Nanocleaner was first mixed with RBC ghosts. Then, various concentrations of MPO were added to the mixtures. RBC-NP was used as a control group. In this case, the relative AChE activity of the RBC ghosts gradually decreased as the MPO concentration (0.01–1000 μg/mL) increased (Fig. 5b). Specifically, there were significant differences in the activities of AChE on the RBC membrane after treatment with 1–100 μg/mL MPO. Within this concentration range, there was less loss of AChE activity in solutions supplemented with Nanocleaner. Compared with

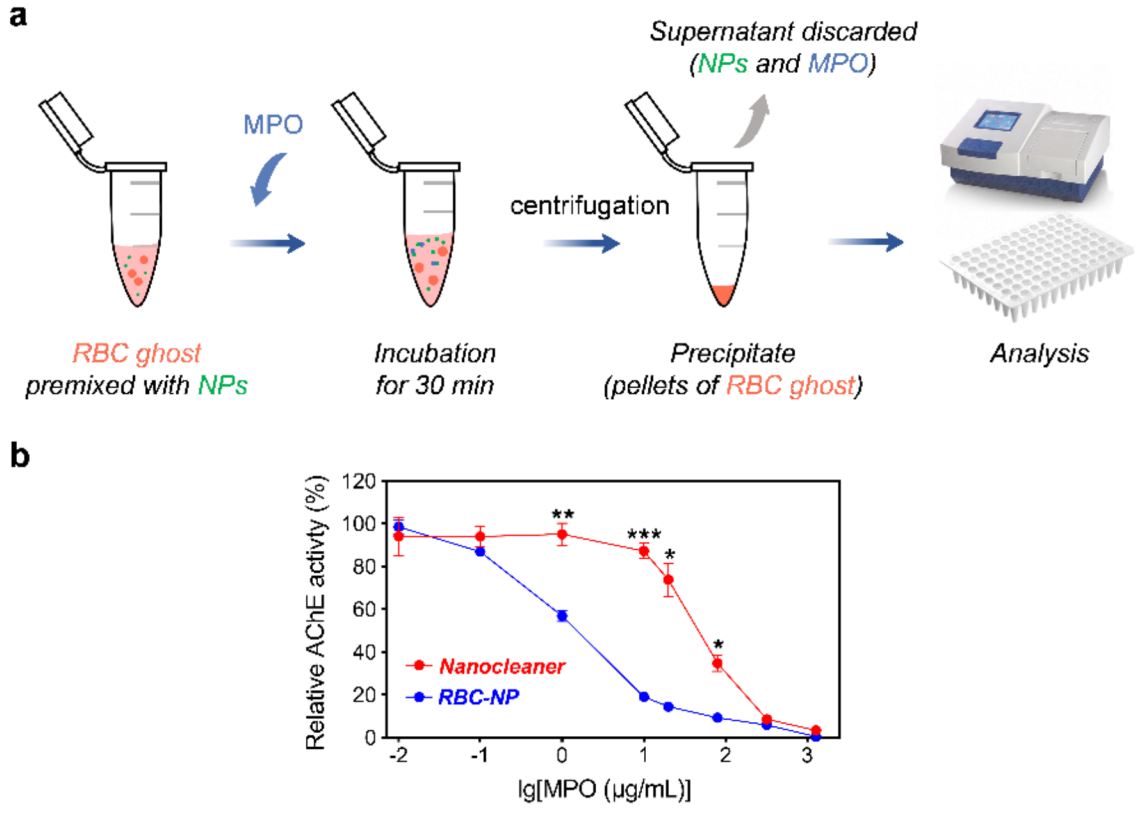

Fig. 5 In vitro neutralization efficacy of Nanocleaner against MPO in a competitive regimen. (**a**) Schematic depicting the experimental design used to evaluate the AChE protective effect of Nanocleaner on RBC ghosts. (**b**) The remaining AChE activity of RBC ghosts in the presence of different concentrations of RBC-NP and Nanocleaner following incubation with various concentrations of MPO for 30 min. Data are presented as the mean ± s.e.m. for each group. *$p < 0.05$, **$p < 0.01$, ***$p < 0.001$

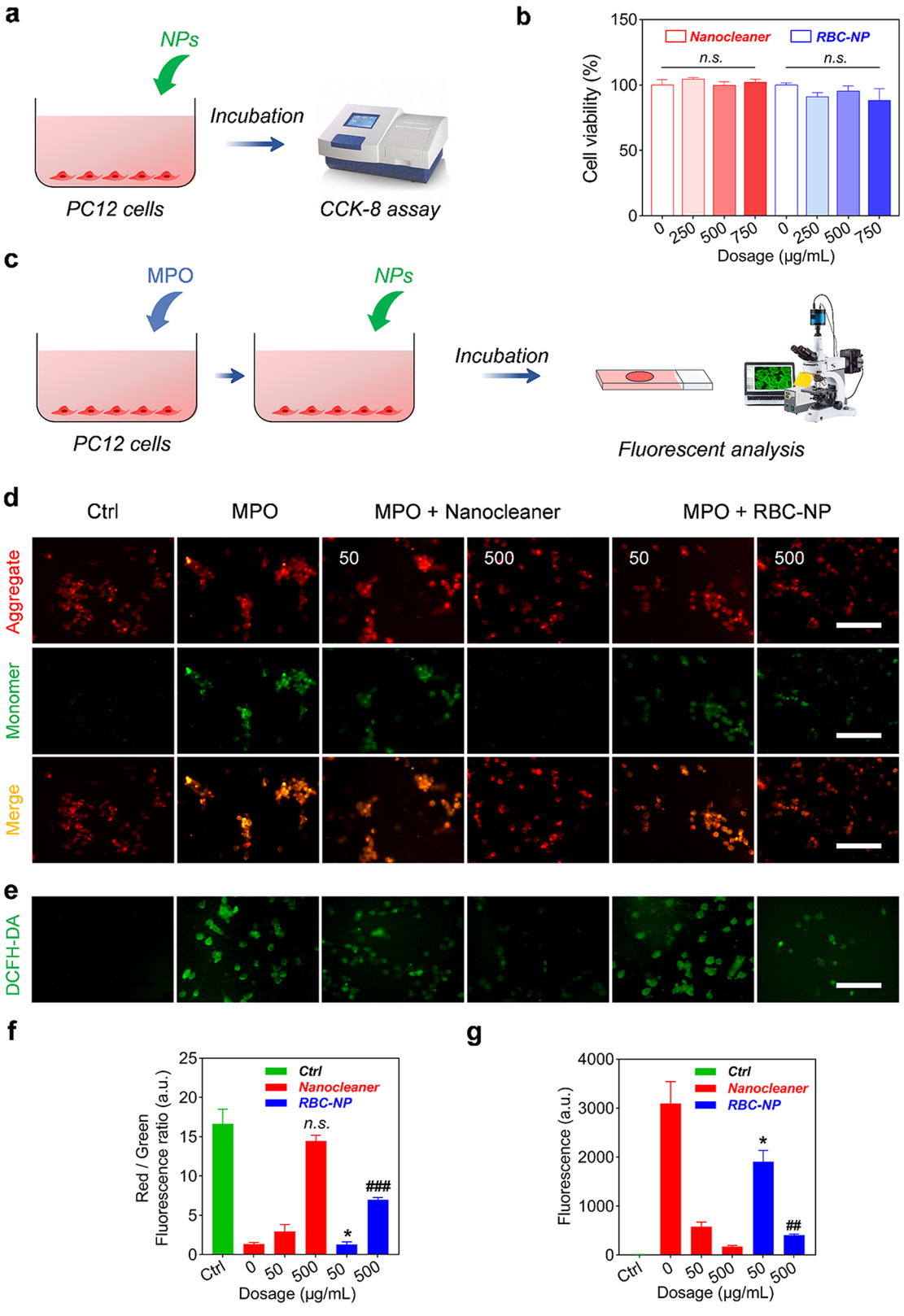

Fig. 6 (See legend on next page.)

(See figure on previous page.)

Fig. 6 In vitro cytoprotection of Nanocleaner. (**a**) Schematic depicting the experimental design used to evaluate the cytocompatibility of Nanocleaner or RBC-NP on PC12 cells. (b) PC12 cell viability after treatment with different concentrations of nanoparticles. The data are presented as the mean ± s.e.m. for each group. *n.s.*: not significant. (**c**) Schematic depicting the experimental design used to evaluate the cytoprotection of PC12 cells by Nanocleaner. (**d**) Representative fluorescence images of PC12 cells coincubated with cationic JC-1 dye. The cells were exposed to PBS (Ctrl), MPO (5 μg/mL), or MPO (5 μg/mL) and incubated with Nanocleaner (50, 500 μg/mL), and the cells were incubated with MPO (5 μg/mL) and RBC-NP (50, 500 μg/mL). Scale bars, 100 μm. (**e**) Representative fluorescence images of PC12 cells coincubated with DCFH-DA dye. The cells were exposed to PBS (Ctrl), MPO (5 μg/mL), MPO (5 μg/mL) incubated with Nanocleaner (50, 500 μg/mL) and MPO (5 μg/mL) incubated with RBC-NP (50, 500 μg/mL). Scale bars, 100 μm. (**f**) Fluorescence intensity of JC-1 dye in different combinations. The data are presented as the mean ± s.e.m. for each group. *n.s.*: not significant vs. Ctrl, $^{*}p < 0.05$ vs. 50 μg/mL Nanocleaner, $^{\#\#\#}p < 0.001$ vs. 500 μg/mL Nanocleaner. (**g**) Fluorescence intensity of DCFH-DA dye in different combinations. The data are presented as the mean ± s.e.m. for each group. $^{*}p < 0.05$ vs. 50 μg/mL Nanocleaner, $^{\#\#}p < 0.01$ vs. 500 μg/mL Nanocleaner

RBC-NP group, AChE activity in Nanocleaner group increased 5-fold under the attack of 10 μg/mL of MPO. Moreover, the shift to the right of the curve reflected that Nanocleaner helped AChE tolerate higher doses of MPO. These results demonstrated that Nanocleaner could effectively compete with RBC ghosts and preserve their AChE activity against MPO.

Biocompatibility of nanocleaner

The biocompatibility of the resulting nanoparticles is essential for their biomedical applications [31]. A cell cytotoxicity experiment was first carried out with a CCK-8 assay (Fig. 6a). NPs at various concentrations had no obvious inhibitory effects on cell proliferation (Fig. 6b), revealing good cytocompatibility.

Then, a hemolysis assay was carried out to evaluate the blood compatibility of Nanocleaner. As expected, the NH_4Cl solution showed hemolytic properties toward RBCs, while no hemolytic phenomenon was observed for either RBC-NP and Nanocleaner (Figure S5). Collectively, these results indicated the desirable biocompatibility of Nanocleaner and RBC-NP.

Cytoprotective effects of nanocleaner

After demonstrating the protective effects of Nanocleaner in vitro, the PC12 neuroendocrine cell line was selected as an experimental cell model to evaluate the protective effects of Nanocleaner. It has been reported that OPs can induce a decrease in the mitochondrial membrane potential [32]. A cationic fluorescent probe, 5,6,6'-tetrachloro-1,1',3,3-tetraethylbenzimidazolylcarbocyanine iodide (JC-1), was applied to investigate the influence of invasive MPO on the mitochondrial membrane potential in neuroendocrine cells. Red fluorescent JC-1 aggregates at higher mitochondrial concentrations, indicating greater mitochondrial membrane potential, and green fluorescent JC-1 monomers at lower mitochondrial concentrations, reflecting lower membrane potential [33–35]. As illustrated in Fig. 6c, the presence of hostile MPO resulted in an obvious reduction in the red fluorescence intensity and an increase in the green fluorescence intensity. Moreover, the intensity of the red fluorescence signal gradually decreased, and the intensity of the green fluorescence signal increased with increasing concentrations of MPO, indicating an imbalance in the membrane potential (Figure S6). MPO-poisoned cells presented green fluorescent signals, indicating severe damage to the cell body. Fortunately, this damage was effectively alleviated with the aid of Nanocleaner and RBC-NP (Fig. 6d). Therefore, it could be concluded that Nanocleaner could realize excellent cytopotection performance with good cytocompatibility. Excessive reactive oxygen species (ROS) production is often accompanied by mitochondrial dysfunction and is closely related to cell apoptosis [36, 37]. To further investigate whether MPO can trigger cellular oxidative stress, the intracellular content of ROS was detected with the H_2DCFDA (DCFH-DA) probe. The results showed that MPO can indeed trigger a significant increase in ROS in PC12 cells (Fig. 6e). However, green fluorescence was obviously reduced by treatment with Nanocleaner (500 μg/mL) and RBC-NP (500 μg/mL), which was equivalent to that of normal cells (Fig. 6g). Overall, the detoxification function of Nanocleaner can significantly attenuate MPO-induced mitochondrial dysfunction and excessive ROS production.

In vivo detoxification experiments in a mouse intoxication model

Toxic OPs represent a great threat to both military and civilian populations [38]. The efficient in vitro protective effect encouraged us to provide proof of concept that Nanocleaner could exert detoxification effects and exploit its therapeutic potential on MPO-induced damage in vivo. A corresponding mouse model of OP intoxication was then established (Fig. 7a). To determine the lethal dose of MPO, a single intraperitoneal injection of various doses of MPO solution (2.7, 2.8, 2.9 and 3.0 mg/kg) was administered, and the survival rate and time of death of the mice were monitored. As expected, the survival rate dramatically decreased as the OP dosage increased. All animals were rapidly poisoned to death within 10 min when the injection dose reached 2.9 mg/kg (LD_{100}) (Figure S7). Next, the mice were injected with MPO at the LD_{100} dose, followed by a single intravenous injection of RBC-NP (50 or 100 mg/kg) or Nanocleaner (0, 50, 100 or 200 mg/kg). Immediately after OP injection, the poisoning symptoms of the mice, including the appearance

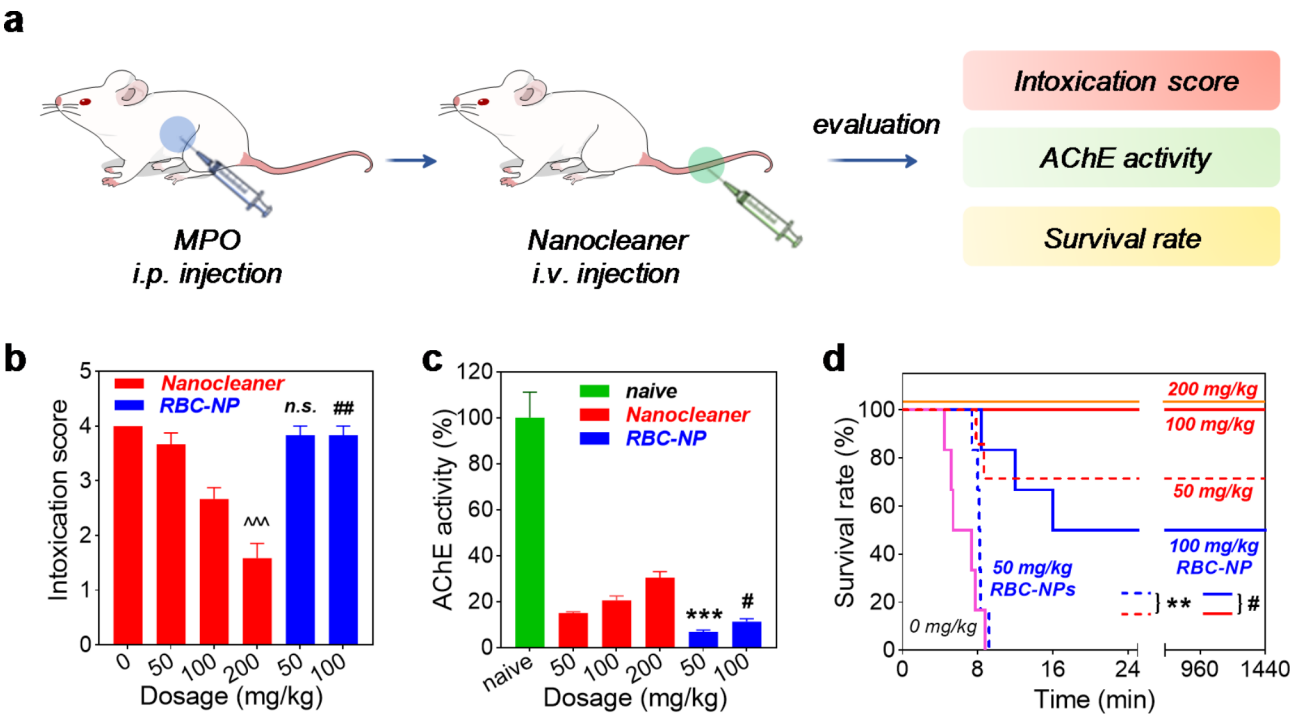

Fig. 7 In vivo neutralization efficacy of Nanocleaner against MPO intoxication. (**a**) Schematic showing the experimental design for in vivo detoxification of MPO. *i.p.*: intraperitoneal, *i.v.*: intravenous. (**b**) Intoxication scores of ICR mice after injection of MPO at the LD_{100} and RBC-NP (50 or 100 mg/kg) or Nanocleaner at various dosages (0, 50, 100, or 200 mg/kg). (**c**) Quantification of blood AChE activity 15 min post-MPO injection. (**d**) Survival rate of ICR mice ($n = 6$) 24 h after injection of MPO at the LD_{100} and RBC-NP (50 or 100 mg/kg) or Nanocleaner at various dosages (0, 50, 100 or 200 mg/kg). The data are presented as the mean ± s.e.m. for each group. *n.s.*: not significant vs. 50 mg/kg Nanocleaner, ^^^: $p < 0.001$ vs. 0 mg/kg Nanocleaner, **: $p < 0.01$ vs. 50 mg/kg Nanocleaner, ***: $p < 0.001$ vs. 50 mg/kg Nanocleaner, $^{\#}$: $p < 0.05$ vs. 100 mg/kg Nanocleaner, $^{\#\#}$: $p < 0.01$ vs. 100 mg/kg Nanocleaner

of salivation, muscle cramping, whole body tremors, and hypoventilation, were observed and carefully recorded on a 0–4 scale (Table S1) [17]. As expected, mice that received a higher dose of Nanocleaner had lower scores than those in the no-treatment groups, indicating the protective effects of Nanocleaner against MPO (Fig. 7b). No deterioration was observed in the following days. Interestingly, at both high and low detoxification doses, the treated mice did not tend to show anticholinergic side effects, including coma, nausea, blurred vision, loss of balance, photophobia, or extreme confusion [39].

Once entered the blood plasma, MPO irreversibly inhibits AChE activity in the blood [18, 40]. Thus, the AChE activity of red blood cells was measured as a biomarker for MPO intoxication. Blood samples were collected from all mice at 15 min post-MPO injection, and the levels of AChE activity were measured. The levels of AChE activity improved as the administered Nanocleaner dose increased (Fig. 7c).

The survival rate of the mice, measured as the percentage of death in the first 24 h after MPO challenge, is summarized in Fig. 7d. No survival benefits were observed when the mice received 50 mg/kg RBC-NP, while two-thirds of the animals survived after treatment with 50 mg/kg Nanocleaner. When the dose of Nanocleaner increased to 100 mg/kg, the survival rate dramatically increased from 66.7 to 100%. In contrast, half of the mice challenged with MPO were still killed after treatment with 100 mg/kg RBC-NP. Considering that the blood volume of mice is approximately 72 mL/kg [41], it can be estimated that the minimum blood concentration of Nanocleaner needed to prevent lethality is 1.39 mg/mL, and at least 2.78 mg/mL could alleviate poisoning symptoms in mice challenged with MPO.

Compared with Nanocleaner group, a similar protective efficacy was observed in OPH groups since the levels of intoxication score, AChE activity and survival rate were improved as the administered OPH dose increased. Despite the improved detoxification capacity, venous administration of biological OPH, especially repeated dosing, might trigger the accelerated blood clearance (ABC) phenomenon [42]. To this end, RBC membrane-coated nanoparticles have been developed to mimic the long circulation time of natural RBCs in an effort, and they serve as an alternative strategy to engineer stealth nanoparticles that have the potential to be more effective than current approaches [20].

In vivo biodistribution, clearance and biosafety of nanocleaner

The in vivo distribution profile and biosafety of Nanocleaner after intravenous administration were evaluated. To assess the organ-level distribution, these nanomaterials were labelled with a fluorescent dye, followed by intravenous administration through the tail vein. The mice were imaged and analysed for fluorescent signals at predetermined time points (3, 24, 48 and 72 h) postinjection (Fig. 8a). At 3 h, the fluorescence signal was inconspicuous because the majority of the nanoparticles were still distributed in the bloodstream. The fluorescent signals of the nanoparticles were detected at 24 h and were still detectable until 72 h (Fig. 8b and Figure S9). When analysed for in vivo distribution per organ, Nanocleaner was distributed mainly in the liver (Fig. 8c). In contrast, nanoparticles were largely retained in the spleen, liver and lung when they were normalized to the organ weight (Fig. 8d and Figure S10). This distribution pattern was consistent with that of other cell membrane-derived nanoparticles [43, 44], implying the recognition and phagocytosis of these nanoparticles by the reticuloendothelial system (RES) [20, 31].

The acute toxicity of Nanocleaner in mice was evaluated after in vivo administration. Nanocleaner was injected intravenously through the tail vein into healthy

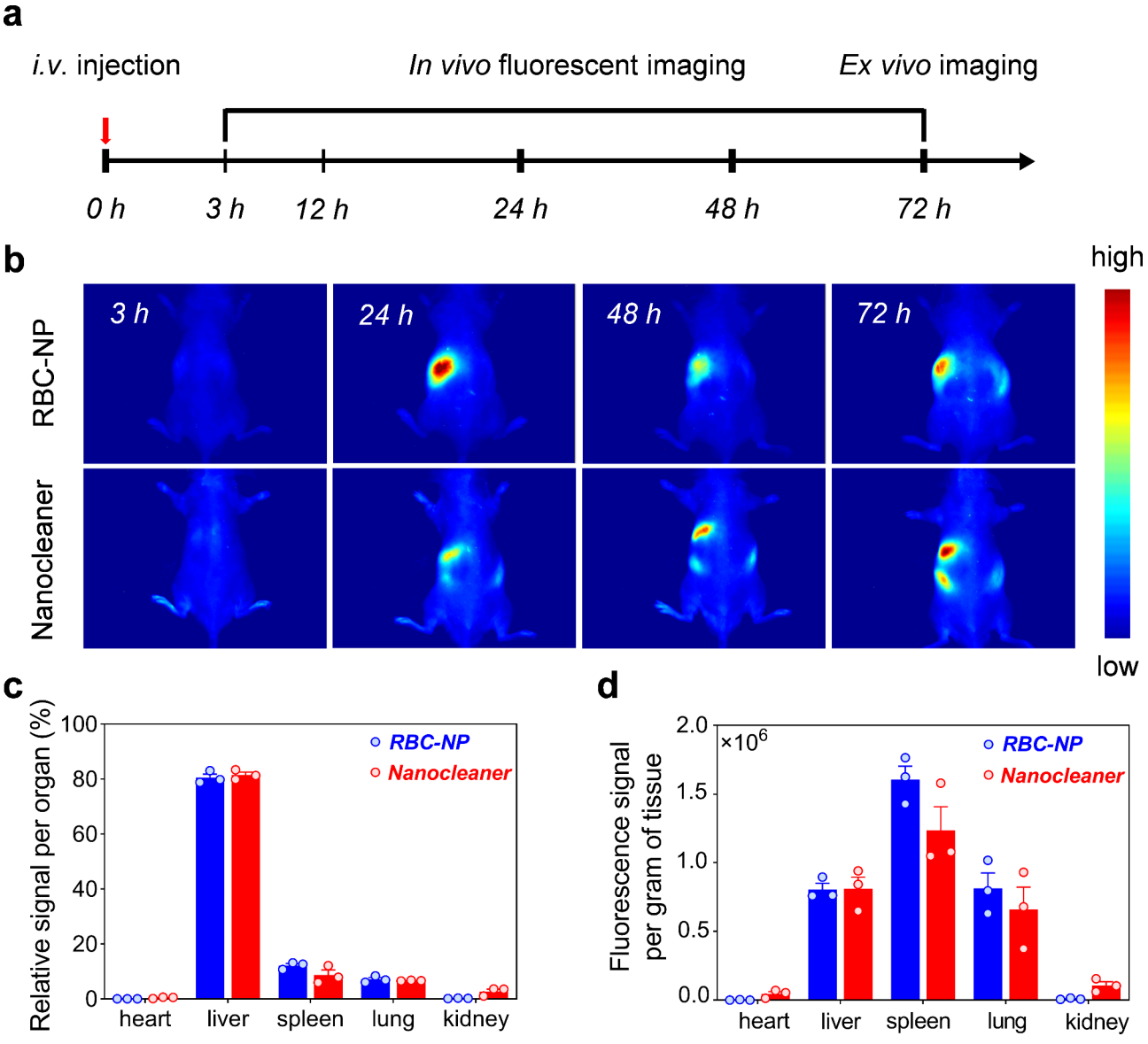

Fig. 8 In vivo biodistribution of Nanocleaner in mice. (**a**) Schematic showing the experimental timeline of fluorescence imaging. (**b**) In vivo fluorescence imaging of mice at various time intervals after intravenous injection of DiD-labelled RBC-NP and Nanocleaner, respectively. (**c**) Quantitative data of fluorescence intensity per organ. (**d**) The relative fluorescence signal per gram of tissue. The data are presented as the mean ± s.e.m. for each group

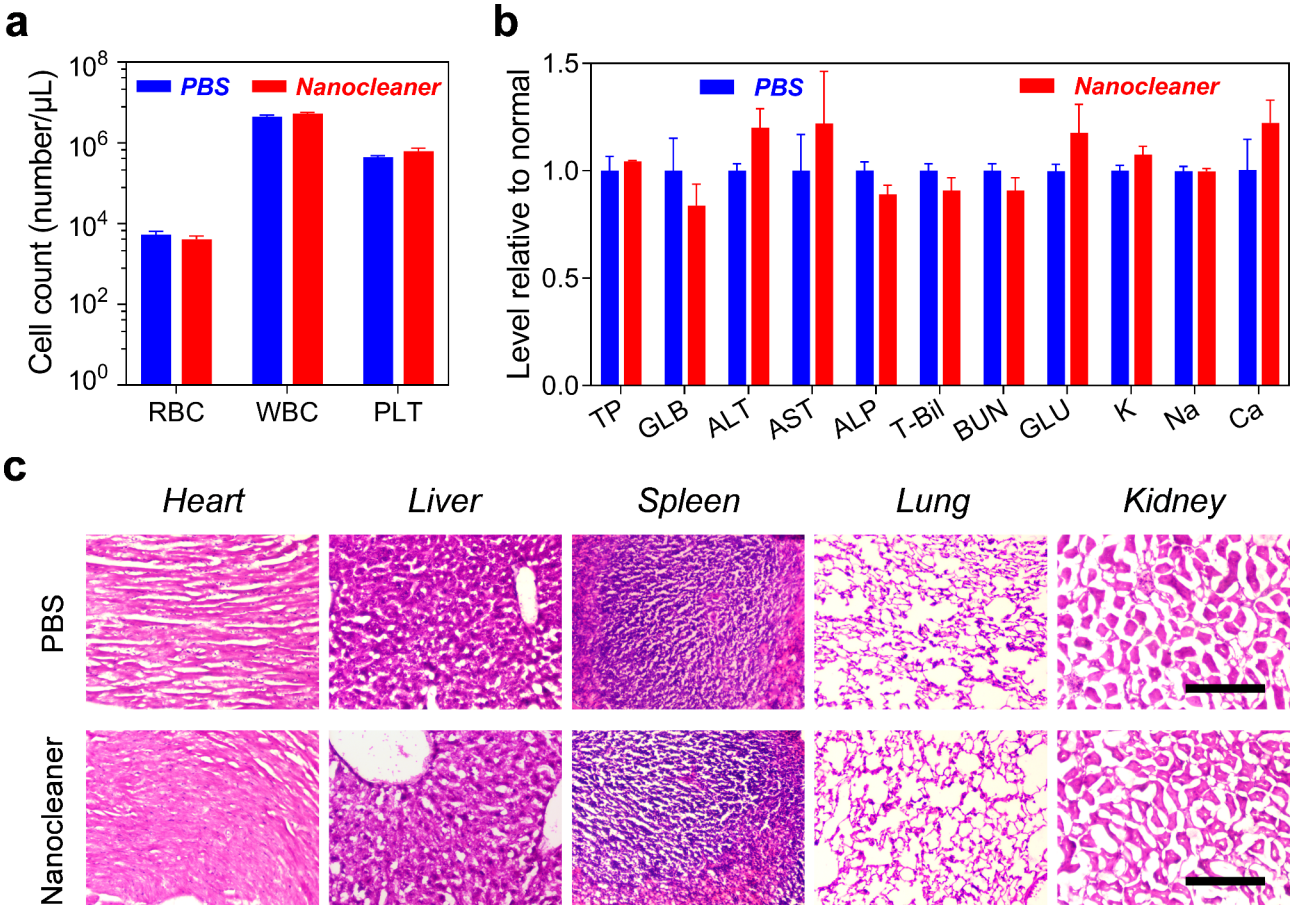

Fig. 9 In vivo biosafety of Nanocleaner. (**a**) Blood cell counts 24 h after intravenous injection of PBS or Nanocleaner ($n = 3$). WBC, white blood cell; RBC, red blood cell; PLT, platelet. (**b**) Blood biochemistry panel analysis after 24 h of intravenous administration of PBS or Nanocleaner ($n = 3$). TP: total protein, GLB: globulin, ALT: alanine transaminase, AST: aspartate aminotransferase, ALP: alkaline phosphatase, T-Bil: total bilirubin, BUN: urea nitrogen, GLU: glucose, K^+: potassium, Na^+: sodium, CA: calcium. (**c**) Histologic examination of major organs (heart, liver, spleen, lung and kidney) at 3 days post administration of PBS and Nanocleaner, respectively. The tissue sections were stained with H&E. Scale bars, 200 μm. In panels **a** and **b**, the data are presented as the mean ± s.e.m. for each group

ICR mice at a dose of 100 mg/kg. PBS injection was used for the control group. The red blood cell, white blood cell and platelet counts at 24 h postadministration were first examined (Fig. 9a). The results showed that the values in the Nanocleaner group were comparable to those in the PBS group. In addition, a panel of blood markers was also tested and was shown in Fig. 9b. The levels were consistent with the baseline levels, without significant differences. Therefore, blood analysis indicated the short-term biosafety of Nanocleaner. The major organs, including the heart, liver, spleen, lung and kidney, of the mice were further harvested, frozen and cut into sections. H&E staining of tissue sections revealed no visible pathological changes in the Nanocleaner group compared to the PBS group (Fig. 9c). Collectively, these experiments provided strong evidence that Nanocleaner has good biosafety.

It deserves to note that, in this work, we established an acute OP intoxication model. In this model, all animals were rapidly poisoned to death within 10 min after MPO exposure. This horrible mortality required the IV administration of Nanocleaner occurring immediately after OP exposure. However, this kind of poisoning was in quite extreme situation and was far different from the actualities. In normal times, OP poisoning is often caused by inhalation, ingestion, and dermal absorption of organophosphorus compounds. The process of poisoning is usually slow and provides sufficient time window for treatment.

In addition, intranasal administration is expected to achieve faster delivery to the brain. The nasal mucosa allows direct drugs delivery to the brain bypassing the blood brain barrier (BBB). Therefore, strategies for improving antidote delivery to the brain by intranasal administration would provide a promising alternative for OP poisoning treatment.

Conclusion

In this study, we designed a biomimetic Nanocleaner with a unique 'targeted binding and catalytic degradation' action mechanism for safe and efficient detoxification against hypertoxic OP. Notably, the resulting Nanocleaner combined the merits of the cell membrane and OPH enzyme and elicited synergistic effects of biological binding and concurrent degradation of MPO, leading to effective dual-action detoxification. As a result, Nanocleaner protected AChE on RBC membranes from OP attack in two regimens. Furthermore, Nanocleaner reduced clinical signs of intoxication and enhanced the survival rate of mice challenged with lethal MPO. In addition, the administration of Nanocleaner to mice resulted in no obvious toxicity. Taken together, the results obtained thus far demonstrate the outstanding detoxification effects of Nanocleaner on OP removal in a mouse model.

Although the use of Nanocleaner in this study is still a proof-of-concept study, its efficient detoxification ability implies its universality and feasibility, allowing for the development of extended detoxification strategies in the future. However, large animal models, such as pigs or even monkeys, should be developed for additional validation of the therapeutic efficacy of Nanocleaner in comparison with that of antidote treatment before human clinical trials. Overall, it is an important step toward the development of treatments for acute OP poisoning.

Supplementary Information

The online version contains supplementary material available at https://doi.org/10.1186/s12951-024-02869-8.

Supplementary Material 1

Acknowledgements

The authors sincerely thank Professor Qiang Zhao of Nankai University, Jie Shi of Tianjin University and Associate Researcher Jing Liu of the Institute of Biomedical Engineering, Chinese Academy of Medical Sciences and Peking Union Medical College for their valuable support and assistance.

Author contributions

KQ, FM: Design, Experiment, Investigation and Writing-original draft. KQ and FM and XL: Cell and Animal experiments. DH, WG and LD: Conceptualization, Methodology. ZL, HZ: review and editing. HY, YP, ZG: Writing-review and editing, Supervision, Funding acquisition. All authors contributed to the article and approved the submitted version.

Funding

This study was financially supported by the National Natural Science Foundation of China (82202331) and the Institute Foundation (2023ZZKY04).

Data availability

No datasets were generated or analysed during the current study.

Declarations

Ethics approval and consent to participate

Protocols of animal experiments included in this study were approved by the policies and guidelines of the Animal Experiments Ethical Committee of the Tianjin Institute of Environmental and Operational Medicine.

Consent for publication

All authors confirmed that this work has not been published before, and was not under consideration for publication elsewhere. All authors have approved the submission of this manuscript to Journal of Nanobiotechnology.

Competing interests

The authors declare no competing interests.

Received: 21 May 2024 / Accepted: 23 September 2024
Published online: 30 September 2024

References

1. Stone R. How to defeat a nerve agent. Science. 2018;359:23.
2. Eddleston M, Buckley NA, Eyer P, Dawson AH. Management of acute organophosphorus pesticide poisoning. Lancet. 2008;371:597–607.
3. Henretig FM, Kirk MA, McKay CA. Hazardous Chemical emergencies and poisonings. N Engl J Med. 2019;380:1638–55.
4. Pang Z, Hu CM, Fang RH, Luk BT, Gao W, Wang F, Chuluun E, Angsantikul P, Thamphiwatana S, Lu W, Jiang X, Zhang L. Detoxification of Organophosphate Poisoning using nanoparticle bioscavengers. ACS Nano. 2015;9:6450–8.
5. Alejo-González K, Hanson-Viana E, Vazquez-Duhalt R. Enzymatic detoxification of organophosphorus pesticides and related toxicants. J Pesticide Sci. 2018;43:1–9.
6. Saxena A, Sun W, Fedorko JM, Koplovitz I, Doctor BP. Prophylaxis with human serum butyrylcholinesterase protects guinea pigs exposed to multiple lethal doses of soman or VX. Biochem Pharmacol. 2011;81:164–9.
7. Ashani Y, Pistinner S. Estimation of the Upper Limit of Human Butyrylcholinesterase Dose required for Protection against organophosphates toxicity: a mathematically based Toxicokinetic Model. Toxicol Sci. 2004;77:358–67.
8. Wales ME, Reeves TE. Organophosphorus hydrolase as an in vivo catalytic nerve agent bioscavenger. Drug Test Anal. 2012;4:271–81.
9. Bigley AN, Xu C, Henderson TJ, Harvey SP, Raushel FM. Enzymatic neutralization of the Chemical Warfare Agent VX: evolution of phosphotriesterase for Phosphorothiolate Hydrolysis. J Am Chem Soc. 2013;135:10426–32.
10. Efremenko EN, Lyagin IV, Klyachko NL, Bronich T, Zavyalova NV, Jiang Y, Kabanov AV. A simple and highly effective catalytic nanozyme scavenger for organophosphorus neurotoxins. J Controlled Release. 2017;247:175–81.
11. Fang RH, Kroll AV, Gao W, Zhang L. (2018) Cell membrane Coating Nanotechnology. Adv Mater 30.
12. Chen Y, Zhang Y, Chen M, Zhuang J, Fang RH, Gao W, Zhang L. Biomimetic nanosponges suppress in vivo lethality induced by the whole secreted proteins of pathogenic bacteria. Small. 2019;15:1804994.
13. Copp JA, Fang RH, Luk BT, Hu CM, Gao W, Zhang K, Zhang L. Clearance of pathological antibodies using biomimetic nanoparticles. Proc Natl Acad Sci U S A. 2014;111:13481–6.
14. Thamphiwatana S, Angsantikul P, Escajadillo T, Zhang Q, Olson J, Luk BT, Zhang S, Fang RH, Gao W, Nizet V, Zhang L. Macrophage-like nanoparticles concurrently absorbing endotoxins and proinflammatory cytokines for sepsis management. Proc Natl Acad Sci U S A. 2017;114:11488–93.
15. Zhang Q, Dehaini D, Zhang Y, Zhou J, Chen X, Zhang L, Fang RH, Gao W, Zhang L. Neutrophil membrane-coated nanoparticles inhibit synovial inflammation and alleviate joint damage in inflammatory arthritis. Nat Nanotech. 2018;13:1182–90.
16. Zhang Q, Honko A, Zhou J, Gong H, Downs SN, Vasquez JH, Fang RH, Gao W, Griffiths A, Zhang L. Cellular Nanosponges inhibit SARS-CoV-2 infectivity. Nano Lett. 2020;20:5570–4.
17. Zhang P, Liu EJ, Tsao C, Kasten SA, Boeri MV, Dao TL, DeBus SJ, Cadieux CL, Baker CA, Otto TC, Cerasoli DM, Chen Y, Jain P, Sun F, Li W, Hung H-C, Yuan Z, Ma J, Bigley AN, Raushel FM, Jiang S. Nanoscavenger provides long-term prophylactic protection against nerve agents in rodents. Sci Transl Med. 2019;11:eaau7091.

18. Lorke DE, Petroianu GA. The experimental oxime K027—a promising protector from organophosphate pesticide poisoning. A review comparing K027, K048, pralidoxime, and obidoxime. Front Neurosci. 2019;13:427.
19. Wang Z, Popowski KD, Zhu D, De Juan Abad BL, Wang X, Liu M, Lutz H, De Naeyer N, DeMarco CT, Denny TN, Dinh P-UC, Li Z, Cheng K. Exosomes decorated with a recombinant SARS-CoV-2 receptor-binding domain as an inhalable COVID-19 vaccine. Nat Biomed Eng. 2022;6:791–805.
20. Hu CM, Zhang L, Aryal S, Cheung C, Fang RH, Zhang L. Erythrocyte membrane-camouflaged polymeric nanoparticles as a biomimetic delivery platform. Proc Natl Acad Sci U S A. 2011;108:10980–5.
21. Zhang H, Luo J, Woodley JM, Wan Y. Confining the motion of enzymes in nanofiltration membrane for efficient and stable removal of micropollutants. Chem Eng J. 2021;421:127870.
22. Ellman GL, Courtney KD, Andres V, Featherstone RM. A new and rapid colorimetric determination of acetylcholinesterase activity. Biochem Pharmacol. 1961;7:88–95.
23. Chen Y, Zhang Y, Zhuang J, Lee JH, Wang L, Fang RH, Gao W, Zhang L. Cell-membrane-cloaked oil nanosponges enable dual-modal detoxification. ACS Nano. 2019;13:7209–15.
24. Ma M, Liu Z, Gao N, Pi Z, Du X, Ren J, Qu X. Self-protecting biomimetic nanozyme for selective and synergistic clearance of peripheral amyloid-β in an Alzheimer's disease model. J Am Chem Soc. 2020;142:21702–11.
25. Shi P, Ju E, Wang J, Yan Z, Ren J, Qu X. Host–guest recognition on photo-responsive cell surfaces directs cell–cell contacts. Mater Today. 2017;20:16–21.
26. Duan X, Chan C, Han W, Guo N, Weichselbaum RR, Lin W. Immunostimulatory nanomedicines synergize with checkpoint blockade immunotherapy to eradicate colorectal tumors. Nat Commun. 2019;10:1899.
27. Hu C-MJ, Fang RH, Copp J, Luk BT, Zhang L. A biomimetic nanosponge that absorbs pore-forming toxins. Nat Nanotech. 2013;8:336–40.
28. Chao MP, Weissman IL, Majeti R. The CD47–SIRPα pathway in cancer immune evasion and potential therapeutic implications. Curr Opin Immunol. 2012;24:225–32.
29. Aubert SD, Li Y, Raushel FM. Mechanism for the hydrolysis of organophosphates by the bacterial phosphotriesterase. Biochemistry. 2004;43:5707–15.
30. Raushel FM. Bacterial detoxification of organophosphate nerve agents. Curr Opin Microbiol. 2002;5:288–95.
31. Almeida JPM, Chen AL, Foster A, Drezek R. In vivo biodistribution of nanoparticles. Nanomedicine. 2011;6:815–35.
32. Xu W, Cai X, Wu Y, Wen Y, Su R, Zhang Y, Huang Y, Zheng Q, Hu L, Cui X, Zheng L, Zhang S, Gu W, Song W, Guo S, Zhu C. Biomimetic single Al-OH site with high acetylcholinesterase-like activity and self-defense ability for neuroprotection. Nat Commun. 2023;14:6064.
33. Elefantova K, Lakatos B, Kubickova J, Sulova Z, Breier A. (2018) Detection of the mitochondrial membrane potential by the Cationic Dye JC-1 in L1210 cells with massive overexpression of the plasma membrane ABCB1 drug transporter. Int J Mol Sci 19.
34. Xu B, Li S, Zheng L, Liu Y, Han A, Zhang J, Huang Z, Xie H, Fan K, Gao L, Liu H. (2022) A Bioinspired Five-Coordinated Single-Atom Iron Nanozyme for Tumor Catalytic Therapy. Advanced Materials 34.
35. Amar SK, Donohue KB, Gust KA. Cellular and molecular responses to ethylparathion in undifferentiated SH-SY5Y cells provide neurotoxicity pathway indicators for organophosphorus impacts. Toxicol Sci. 2023;191:285–95.
36. Rao S, Lin Y, Du Y, He L, Huang G, Chen B, Chen T. Designing multifunctionalized selenium nanoparticles to reverse oxidative stress-induced spinal cord injury by attenuating ROS overproduction and mitochondria dysfunction. J Mater Chem B. 2019;7:2648–56.
37. Ben Salem I, Boussabbeh M, Bacha H, Abid S. Dichlorvos-induced toxicity in HCT116 cells: involvement of oxidative stress and apoptosis. Pestic Biochem Physiol. 2015;119:62–6.
38. Yanagisawa N, Morita H, Fau - Nakajima T, Nakajima T. Sarin experiences in Japan: acute toxicity and long-term effects.
39. Collamati A, Martone AM, Poscia A, Brandi V, Celi M, Marzetti E, Cherubini A, Landi F. Anticholinergic drugs and negative outcomes in the older population: from biological plausibility to clinical evidence. Aging Clin Exp Res. 2016;28:25–35.
40. Petroianu G, Kalasz H. Comparison of the ability of pyridinium aldoximes to reactivate human RBC cholinesterases inhibited by ethyl- and methylparaoxon. COC. 2007;11:1624–34.
41. Vacha J. Blood volume in inbred strain BALB/c, CBA/J and C57BL/10 mice determined by means of 59Fe-labelled red cells and 59Fe bound to transferrin. Physiol Bohemoslov. 1975;24:413–9.
42. Mima Y, Hashimoto Y, Shimizu T, Kiwada H, Ishida T. Anti-PEG IgM is a major contributor to the Accelerated Blood Clearance of Polyethylene Glycol-Conjugated Protein.
43. Zhu X, Wang J, Cai L, Wu Y, Ji M, Jiang H, Chen J. Dissection of the antibacterial mechanism of zinc oxide nanoparticles with manipulable nanoscale morphologies. J Hazard Mater. 2022;430:128436.
44. Zelepukin I, Yaremenko A, Shipunova V, Babenyshev A, Balalaeva I, Nikitin P, Deyev S, Nikitin M. Nanoparticle-based drug delivery via RBC-hitchhiking for the inhibition of lung metastases growth. Nanoscale. 2019;11:1636–46.

Publisher's note